Phase Behavior of Mixed Self-Assembled Monolayers of Alkanethiols on Au(111): A Configurational-Bias Monte Carlo Simulation Study

ARTICLE *in* LANGMUIR · NOVEMBER 2001

Impact Factor: 4.46 · DOI: 10.1021/la0108151

4 AUTHORS, INCLUDING:

Jian Zhou
South China University of Technology
84 PUBLICATIONS **1,592** CITATIONS
SEE PROFILE

Melvin T Zin
University of Washington Seattle
16 PUBLICATIONS **353** CITATIONS
SEE PROFILE

Phase Behavior of Mixed Self-Assembled Monolayers of Alkanethiols on Au(111): A Configurational-Bias Monte Carlo Simulation Study

Abhijit V. Shevade,[†,‡] Jian Zhou,[§] Melvin T. Zin,[§] and Shaoyi Jiang*[,§]

Department of Chemical Engineering, Kansas State University, Manhattan, Kansas 66506, and Department of Chemical Engineering, University of Washington, Seattle, Washington 98195

Received June 4, 2001. In Final Form: September 4, 2001

We report a configurational-bias Monte Carlo simulation study to investigate the effect of chain length, system size, and temperature on the preferential adsorption and phase behavior of mixed self-assembled monolayers (SAMs) of alkanethiols on Au(111). Simulations were performed in both semigrand canonical and canonical ensembles. The semigrand canonical simulations were carried out at conditions corresponding to low concentration of $HS(CH_2)_8CH_3-HS(CH_2)_9CH_3$ and $HS(CH_2)_8CH_3-HS(CH_2)_{10}CH_3$ alkanethiol mixtures in solutions at 300 and 373 K. The canonical ensemble simulations were performed at 300 K for a fixed composition of $HS(CH_2)_9CH_3-HS(CH_2)_{9+n}CH_3$ mixed SAMs, where $n = 1, 2, ..., 10$. Continuous and discrete models were used in these simulations for describing the alkanethiol chains, and an analytical potential was used to model their interactions with the gold surface. Results show the preferential adsorption of long chains on the surface over in the solution and the occurrence of phase segregation when the two components in the mixed SAMs differ by more than three carbon atoms at a fixed surface composition (1:1). Calculated translational, orientational, and conformational orders of the mixed SAMs reveal a more pseudocrystalline structure consisting of closely packed and inclined chains at 300 K than at 373 K. The effect of system size on various properties was also studied.

1. Introduction

The class of molecular assemblies, such as self-assembled monolayers (SAMs), provides viable means of controlling both physical and chemical properties of a solid surface. The fabrication of nanoscale structures using SAMs has recently attracted much attention due to their scientific importance and potential applications in molecular electronics, biocompatible materials, and biosensors.[1−6] SAMs are formed by spontaneous adsorption of self-assembling molecules from either a single component or a mixture on a solid substrate.[7] Examples of SAM systems include alkanethiols or dialkyl disulfides on noble metals such as gold and silver, organosilicon on hydroxylated silicon wafers, and carboxylic acids on aluminum oxide.[7] Mixed SAMs are very promising since they can be used to systematically alter the chemical and structural complexities of a surface by varying chain length, tail group, and composition.[8] The ability to control surface properties at the molecular level makes SAMs excellent platforms for studies of the interactions between man-made surfaces and biological systems.

The knowledge of molecular behavior is important for the design of novel materials with desired properties. Early electronic diffraction studies of alkanethiol monolayers on Au(111) have shown a hexagonal symmetry of sulfur atoms with a sulfur−sulfur spacing of 0.497 nm. A scanning tunneling microscopy study of alkanethiols on Au(111) showed a hexagonal lattice consistent with a $(\sqrt{3} \times \sqrt{3})R30°$ structure.[9,10] Molecular dynamics simulations are often performed to study pure SAM systems.[11−17] There are a few Monte Carlo (MC) simulation studies of structural properties, domain formation, and mechanical relaxation reported for single-component SAMs in a canonical (NVT) ensemble.[18,19] For mixed SAMs, to the best of our knowledge, there is only one MC study for a realistic SAM model that focused on the phase segregation of $HS(CH_2)_9CH_3-HS(CH_2)_{19}CH_3$ alkanethiol mixtures at a fixed surface composition and for a small system size.[20] Mizutani et al.[21] have also reported MC

* To whom correspondence should be addressed. E-mail: sjiang@u.washington.edu.

† Current address: Jet Propulsion Laboratory, California Institute of Technology, Pasadena, CA 91109.

‡ Kansas State University.

§ University of Washington.

(1) Mirksich, M.; Whitesides, G. M. *Annu. Rev. Biophys. Biomol. Struct.* **1996**, *25*, 55.

(2) Allara, D. L.; Dunbar, T. D.; Weiss, P. S.; Bumm, L. A.; Cygan, M. T.; Tour, J. M.; Reinerth, W. A.; Yao, Y. T.; Kozaki, M.; Jones, L. *Ann. N. Y. Acad. Sci.* **1998**, *852*, 349.

(3) Tengvall, P.; Lundstorm, I.; Liedberg, B. *Biomaterials* **1998**, *19*, 407.

(4) Tidwell, C. D.; Ertel, S. I.; Ratner, B. D.; Tarasevinch, B. J.; Atre, S.; Allara, D. L. *Langmuir* **1997**, *13*, 3404.

(5) Zamborini, F. P.; Crook, R. M. *Langmuir* **1998**, *14*, 3249.

(6) Haussling, L.; Ringsdorf, H.; Schmitt, F. J.; Knoll, W. *Langmuir* **1991**, *7*, 1837.

(7) Ulman, A. *Chem. Rev.* **1996**, *96*, 1533.

(8) (a) Bain, C. D.; Evall, J.; Whitesides, K. E. *J. Am. Chem. Soc.* **1989**, *111*, 7155. (b) Bain, C. D.; Whitesides, G. M. *J. Am. Chem. Soc.* **1989**, *111*, 7164.

(9) Widrig, C. A.; Alves, C. A.; Porter, M. D. *J. Am. Chem. Soc.* **1991**, *113*, 2805.

(10) Takano, H.; Kenseth, J. R.; Wong, S.; O'Brien, J. C.; Porter, M. D. *Chem. Rev.* **1999**, *99*, 2845.

(11) Hautman, J.; Klein, M. *J. Chem. Phys.* **1989**, *91* (8), 4994.

(12) Hautman, J.; Klein, M. *J. Chem. Phys.* **1990**, *93* (10), 7483.

(13) Mar, W.; Klein, M. L. *Langmuir* **1994**, *10*, 188.

(14) Sprik, M.; Delamarche, E.; Michel, B.; Rothlisberger, U.; Klein, M. L.; Wolf, H.; Ringsdorf, H. *Langmuir* **1994**, *10*, 4116.

(15) Tupper, K. J.; Brenner, D. W. *Langmuir* **1994**, *10*, 2335.

(16) Bonner, T.; Barato, A. *Surf. Sci.* **1997**, *377*, 1082.

(17) Leng, Y. S.; Jiang, S. *J. Chem. Phys.* **2000**, *113*, 8800.

(18) Siepmann, I.; McDonald, I. R. *Mol. Phys.* **1993**, *79* (3), 457.

(19) (a) Siepmann, I.; McDonald, I. R. *Langmuir* **1993**, *9*, 2351. (b) Siepmann, I. *Tribol. Lett.* **1995**, *1*, 191. (c) Siepmann, I.; McDonald, I. R. *Phys. Rev. Lett.* **1993**, *70* (4), 453.

10.1021/la0108151 CCC: $20.00
Published on Web 10/24/2001

studies for binary components using a simple isotropic rodlike chain model. The relationship between surface and solution compositions and the effect of chain length difference on phase segregation in mixed SAMs has been of great interest.[8,22−25] However, we know of no molecular simulation study targeting these issues. In this work, we report a configurational-bias Monte Carlo (CBMC) simulation study performed in both semigrand canonical and canonical ensembles to study the preferential adsorption and phase behavior of mixed alkanethiol SAMs. The configurational-bias semigrand canonical ensemble MC simulations (CBSGCMC) were carried out at 300 and 373 K for $HS(CH_2)_8CH_3-HS(CH_2)_9CH_3$ and $HS(CH_2)_8CH_3-HS(CH_2)_{10}CH_3$ alkanethiol mixtures. These mixtures hereafter will be referred to as C_9-C_{10} and C_9-C_{11}, respectively. The objective is to study the preferential adsorption of mixed SAMs so as to predict the surface compositions of mixed SAMs on Au(111) at different bulk compositions. The effect of chain length difference on domain formation in mixed SAMs was investigated by performing CBMC simulations in the canonical ensemble at a fixed composition of mixed SAMs (1:1). The mixed SAMs investigated for domain formation include $HS(CH_2)_9CH_3-HS(CH_2)_{9+n}CH_3$ mixtures, where $n = 1, 2, 3, ..., 10$. In the subsequent sections, potential models for fluid−fluid and solid−fluid interactions are discussed in section 2, while section 3 deals with the simulation methodology and results are presented in section 4.

2. Potential Models

The total potential energy of a given molecule can be written as a superposition of short-range valence ($U_{valence}$) and long-range nonbonded interactions ($U_{nonbond}$):

$$U_{total} = U_{valence} + U_{nonbond} \quad (1)$$

where the valence (or internal) terms consist of bond stretch (U_{bond}), bond-angle bending (U_{bend}), and dihedral angle torsion ($U_{torsion}$) terms

$$U_{valence} = U_{bond} + U_{bend} + U_{torsion} \quad (2)$$

while the nonbond (or external) interactions consist of van der Waals (U_{vdw}) and electrostatic (U_Q) terms

$$U_{nonbond} = U_{vdw} + U_Q \quad (3)$$

The U_{vdw} term takes into account intermolecular interactions and interactions between atoms that are separated by three or more bonds within a chain. The atoms of a methyl ($-CH_3$)-terminated alkanethiol chain are assumed to have no charge. Therefore, the Coulombic term (U_Q) has no contribution to eq 3. In the following sections, a detailed account of the models used for fluid−fluid and solid−fluid interactions for alkanethiol chains on Au(111) is discussed.

2.1. Fluid−Fluid Interactions. The united-atom model by Hautman and Klein[11] was used to model alkanethiol chains. Accordingly, a C_9 alkanethiol chain consists of a sulfur atom, eight methylene ($-CH_2$) groups, and a terminal methyl ($-CH_3$) tail group (10 pseudoatoms overall). Similarly, the C_{10} and C_{11} alkanethiols have 11 and 12 pseudoatoms, respectively. For simulations, how the carbon backbone is modeled is of great importance. Two models, discrete and continuous,[18] describe the flexibility of the carbon backbone. The atoms in both models are assumed to be connected by rigid bonds, with carbon−carbon and sulfur−carbon bonds fixed at 0.153 and 0.182 nm, respectively. The discrete model limits the flexibility of the carbon chain, with the CCC and SCC angles fixed at $\theta_{CCC} = 109.87°$ and $\theta_{SCC} = 114.4°$, respectively, and the torsion angles (ϕ) constrained to the minima (0, +120, −120) in the Ryckaert−Bellmans potential.[26] The continuous model uses the harmonic potential for bond-angle bending and the full Ryckaert−Bellmans potential for torsion. The bond-angle bending (U_{bend}) has the form[11]

$$U_{bend}(\theta) = 0.5k_\theta(\theta - \theta_0)^2 \quad (4)$$

where θ is the C−C−C or S−C−C angle, while k_θ and θ_0 are the corresponding force constant and equilibrium angle, respectively. The Ryckaert−Bellmans torsion potential ($U_{torsion}$) has the form[11]

$$U_{torsion}(\phi) = a_0 + a_1\cos(\phi) + a_2\cos^2(\phi) + a_3\cos^3(\phi) + a_4\cos^4(\phi) + a_5\cos^5(\phi) \quad (5)$$

where ϕ is the torsion angle and a_0, ..., a_5 are constants. Parameters in eqs 4 and 5 are listed in Table 1a,b, respectively. Coefficients for the torsion potential listed in Table 1b are for hydrocarbons but are also assumed applicable for torsion angles involving sulfur atoms.[18] Of the two models, the continuous model is more realistic while the discrete model is more computationally efficient. In the present study, the continuous model was used for simulations performed in the semigrand canonical ensemble while the discrete model was used for simulations carried out in the canonical ensemble. Pseudoatoms on different chains and those on the same chain (separated by more than three bonds) interact with each other via a cut and shifted Lennard−Jones (LJ) potential

$$U_{ij} = \begin{cases} u(r) - u(r_c) & r \le r_c \\ 0 & r > r_c \end{cases} \quad (6)$$

where r_c is the cutoff (in this work, $4.5\sigma_{ij}$). Parameters for the LJ potential are listed in Table 2. Cross parameters were calculated by the Lorentz−Berthelot (LB) rule.

Table 1. Parameters for Bending and Torsion Potentials

(a) Parameters for Bending Potentials

parameter	C−C−C	S−C−C
k_θ (kJ/mol)/(deg)^2	1 705 828.25	1 705 828.25
θ_0 (deg)	109.5	114.4

(b) Parameters for Torsion Potentials

parameter	X−C−C−X (kJ/mol)
a_0	9.2784
a_1	12.1550
a_2	−13.1195
a_3	−3.0595
a_4	26.2389
a_5	−31.4934

(20) Siepmann, I.; McDonald, I. R. *Mol. Phys.* **1992**, *75* (2), 255.
(21) Mizutani, W.; Ishida, T.; Tokumoto, H. *Appl. Surf. Sci.* **1998**, *130*, 792.
(22) Folker, J. P.; Laibinis, P. E.; Whitesides, G. M. *J. Phys. Chem.* **1994**, *98*, 563.
(23) Bumm, L. A.; Arnold, J. J.; Charles, L. F.; Dunbar, T. D.; Allara, D. L.; Weiss, P. S. *J. Am. Chem. Soc.* **1999**, *121*, 8017.
(24) Tamada, K.; Hara, M.; Sasabe, H.; Knoll, W. *Langmuir* **1997**, *13*, 1558.
(25) Chen, S.; Li, L.; Boozer, C.; Jiang, S. *Langmuir* **2000**, *16*, 9287.
(26) Ryckaert, J. P.; McDonald, I. R.; Klein, M. L. *Mol. Phys.* **1989**, *67*, 657.

Table 2. Parameters for LJ Fluid−Fluid Potentials

group	σ (nm)	ϵ (kJ/mol)
CH_3	0.3905	0.7325
CH_2	0.3905	0.4938
S	0.355	1.0476
S[a]	0.425	1.6628

[a] Parameter for sulfur−sulfur interactions only.

Table 3. Parameters for Solid−Fluid Potentials

group	$C_{12} \times 10^{-12}$ (nm^{12} kJ/mol)	$C_3 \times 10^{-3}$ (nm^3 kJ/mol)	z_0 (nm)
CH_3	283 507.4	172.93	0.086
CH_2	232 792.0	142.16	0.086
S	339 959.46	1501.51	0.0269

2.2. Solid−Fluid Interactions. Interactions between pseudoatoms of an alkanethiol chain and a flat Au(111) surface are represented by a 12−3 potential[11]

$$U_{sf} = \frac{C_{12}}{(z - z_0)^{12}} - \frac{C_3}{(z - z_0)^3} \tag{7}$$

where z is the distance of pseudoatoms from the gold surface while C_{12}, C_3, and z_0 are constants for pseudoatoms of an alkanethiol chain. The parameters are listed in Table 3. The 12−3 potential is used because it better represents the chemisorbed sulfur because of its narrower attractive well as compared to the 9−3 potential.

3. Simulation Methodology

In simulations, especially those involving chain molecules, achieving configurational equilibrium is very crucial; that is, different conformations of chain molecules are sampled in correct statistical weight.[27] Hence, we incorporate the configurational-bias scheme in MC simulations involving SAMs. Full coverage of alkanethiol SAMs on a gold surface is known to occur for a wide range of alkanethiol concentrations (ranging from micromoles to millimoles) in alcoholic solutions.[22] Thus, CBMC simulations in the semigrand canonical ensemble[28] are well-suited for studying the relationship between surface and bulk compositions for mixed SAMs. CBMC simulations in the canonical ensemble at a fixed surface composition are well-suited for investigating phase segregation in mixed SAMs.[20]

CBMC simulations of mixed SAMs in the canonical ensemble are performed by sampling configuration space with translation, rotation, configurational-bias, and chain interconversion moves.[20] In the chain interconversion move, an attempt is made to change identities of randomly chosen two chains (one of each type), thus keeping the number of chains of each component constant. CBSGCMC simulations are performed by sampling both configurations and compositions of a mixture at a constant number of particles. Exploration of the configuration space is performed as in the canonical ensemble simulation while compositions are altered by changing the identity of a molecule at a fixed ratio of fugacities (known as swap). For CBSGCMC simulations of mixed SAMs, solvent molecules were not considered because they were much less competitive to adsorption on the gold surface as compared to alkanethiol chains. The fugacity of an alkanethiol chain in the solution can be calculated using Henry's law. Previous investigations[29] have shown that Henry's constants of alkanethiols whose chain lengths differ by one or two carbon atoms are not much different. Hence, in the present CBSGCMC simulations of $HS(CH_2)_8CH_3$−$HS(CH_2)_9CH_3$ and $HS(CH_2)_8CH_3$−$HS(CH_2)_{10}CH_3$ alkanethiol mixtures, Henry's constants of alkanethiol chains were assumed to cancel out in the swap criteria, which involves the ratio of fugacities. The random moves involved for the semigrand canonical (translation/rotation/configurational-bias/swap) and canonical ensemble MC simulations (translation/rotation/configurational-bias/chain interconversion) of mixed SAMs were done with equal probability. In addition, at each simulation step, the type of chain in the mixture was chosen with equal probability. Various random moves used in simulations are discussed in the Appendix.

Table 4. CBMC Simulation Conditions

	semigrand canonical		canonical
model	continuous	continuous	discrete
cell size (nm)	4.474 × 4.305	8.948 × 8.61	24.855 × 8.61
number of chains	90	360	1000
temperature (K)	300 and 373	300 and 373	300

A CBMC simulation code was developed for both ensembles and tested for several systems for which simulation results have been reported previously: pure SAMs of $HS(CH_2)_{15}CH_3$ and mixed SAMs of $HS(CH_2)_9CH_3$−$HS(CH_2)_{19}CH_3$ on Au(111).[18,20] All results reported for these cases were reproduced. For the current study, periodic boundary conditions were applied in x and y directions. Runs were for 3.5 million steps for both simulations and were performed on SGI O2 workstations. Simulation conditions are given in Table 4.

4. Results and Discussion

The CBSGCMC simulations were carried out for C_9−C_{10} and C_9−C_{11} alkanethiol mixtures by varying bulk compositions of chains in the solution. The equilibrium process in the simulation was monitored by examining the composition of long chains in SAMs and trends in the mean system tilt (θ_s), the molecular tilt (θ_m), and the total energy (U_{tot}). By definition, the mean system tilt (θ_s) is the angle between the z-axis and the vector connecting the head and tail groups. The mean molecular tilt (θ_m) is defined with respect to vectors passing through the centers of bonds connecting adjacent methylene groups in a given molecule.[18] The difference between θ_s and θ_m reflects the heterogeneity in the system. Normally, for chains with fewer defects, the difference is close to 1°. For the characterization of conformational order, torsion angles between −60 and 60° are described as trans while others are described as gauche.

Figure 1 shows the surface ($x_{C9,SAM}$) vs bulk ($x_{C9,bulk}$) composition relationship for C_9−C_{10} and C_9−C_{11} mixtures at 300 K. The composition of each component in the SAMs was calculated based on the number of chains present at equilibrium. For the C_9−C_{10} mixture, it can be seen that the composition of short chains in the SAMs is about 0.1 for $x_{C9,bulk} = 0.5$ and increases to about 0.45 at $x_{C9,bulk} = 0.9$. As shown in Figure 1, a similar trend can be seen for the C_9−C_{11} mixture. However, the surface vs bulk composition curve in this case drops considerably to lower values. Thus, it can be seen that long chains are preferentially adsorbed over the entire range of bulk compositions for both cases. Experimental studies in this

(27) (a) Frenkel, D.; Smit, B. *Understanding Molecular Simulation*; Academic Press: San Diego, 1996. (b) Siepmann, I.; Frenkel, D. *Mol. Phys.* **1992**, *75*, 59.

(28) Kofke, D.; Glandt, E. D. *Mol. Phys.* **1988**, *64*, 1105.

(29) Przyjanzy, A.; Janicki, W.; Chrzanowski, W.; Staszewski, R. *J. Chromatogr.* **1983**, *280*, 249.

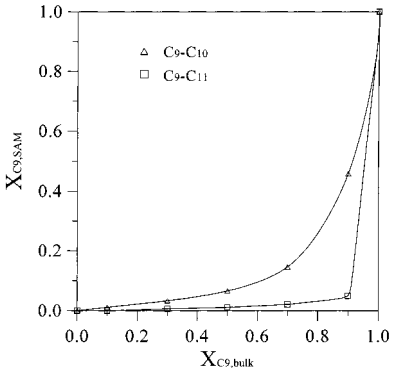

Figure 1. Surface ($x_{C9,SAM}$) vs bulk ($x_{C9,bulk}$) compositions of C_9-C_{10} and C_9-C_{11} mixtures for systems containing 90 chains at 300 K.

regard have focused on mixed SAMs formed by coadsorption from alkanethiol mixtures having various chain lengths, terminal groups, and solvents.[8,22,25] These studies have revealed that thermodynamic cohesive interactions between hydrocarbon chains favor the adsorption of longer chains and that the composition of monolayers adsorbed from a solution containing thiol mixtures is determined mainly by thermodynamic equilibrium.[8] We performed a detailed evaluation of the energy difference caused by the increase of one carbon atom as in the case of the C_9-C_{10} mixture. It was found that the energy contribution due to the addition of an extra ($-CH_2$) group was about 7−9 kJ/mol. This value is consistent with that previously reported.[35,36] Whenever a long chain swaps a short chain, energetics favors the long chain. In experiments, kinetics could play a role in the formation of SAMs. For example, uniform mixed SAMs were prepared using a "kinetically trapped" method by increasing the solution temperature for self-assembly.[25] Simulation results in our case represent the thermodynamic limit whereas kinetics involved in the process is not taken into consideration. Figure 2a shows the chain configuration of the C_9-C_{10} mixture for $x_{C9,bulk} = 0.9$ at 300 K. It can be seen that the chain atoms are denser and more ordered near the gold surface than near the bulk. The orientational and conformational orders of the C_9-C_{10} and C_9-C_{11} mixtures for $x_{C9,bulk} = 0.9$ at 300 K are given in Table 5. The chains are tilted 27−28° on average. About 2% of gauche defects were observed. The mean distances from the surface to the sulfur (z_{head}) and to the terminal carbon atom (z_{tail}) are also given in Table 5. The values of z_{tail} provide a good estimate of monolayer thickness.

The effect of temperature on the surface vs bulk composition relationship for the C_9-C_{10} mixture is shown in Figure 3 for temperatures at 300 and 373 K. As expected, the composition of short chains on the surface increases with temperature.[22] The chain configuration of the C_9-C_{10} mixture for $x_{C9,bulk} = 0.9$ at 373 K is shown in Figure 2b. At 373 K, more defects were observed. At higher

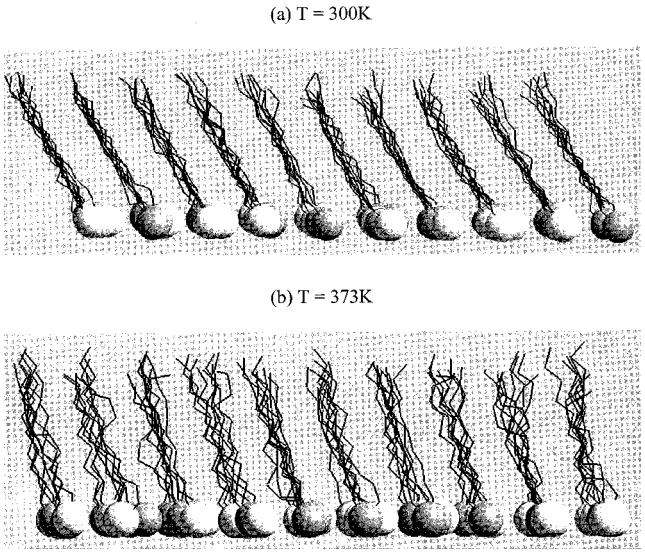

Figure 2. Equilibrium chain configuration viewed from the side for the C_9-C_{10} SAMs containing 90 chains for $x_{C9,bulk} = 0.9$ at (a) 300 and (b) 373 K. Gray and white spheres represent sulfur atoms of C_9 and C_{10}, respectively.

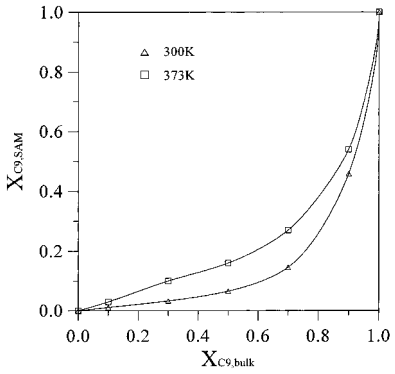

Figure 3. Surface ($x_{C9,SAM}$) vs bulk ($x_{C9,bulk}$) compositions of C_9-C_{10} mixtures for systems containing 90 chains at 300 and 373 K.

Table 5. Equilibrium Properties of C_9-C_{10} and C_9-C_{11} SAMs for a Bulk Composition of $x_{C9,bulk} = 0.9$ at 300 K for 90 Chains

	C_9-C_{10}	C_9-C_{11}
$\langle x_{C9,SAM} \rangle$	0.45	0.05
$\langle \theta_s \rangle$ (deg)	27.19	26.78
$\langle \theta_m \rangle$ (deg)	28.13	27.37
$\langle z_{head} \rangle$ (nm)	0.240	0.241
$\langle z_{tail} \rangle$ (nm)	1.353	1.471
$\langle U_{tot} \rangle$ (kJ mol^{-1})	−170.78	−177.26
gauche (%)	2.08	2.75

temperatures, there are larger deviations of torsion angles from their equilibrium values. This results in less ordered configurations at higher temperatures. Table 6 gives the effect of temperature on the configurational properties of the C_9-C_{10} SAMs containing 90 chains for $x_{C9,bulk} = 0.9$. It can be seen that as temperature increases both the system and the molecular tilt angles decrease and their difference increases, justifying the fact that the number of gauche defects increases with temperature.[37] A higher temperature of 373 K results in larger changes in tilt direction and reorientational motion about the chain axis, smaller tilt angles, thicker monolayer, and higher density of gauche defects. The increase of

(30) Allen, M. P.; Tildesley, D. J. *Computer Simulation of Liquids*; Clarendon Press: Oxford, 1987.
(31) (a) Cracknell, R. F.; Nicholson, D. *J. Chem. Soc., Faraday Trans.* **1994**, *90*, 1487. (b) Cracknell, R. F.; Nicholson, D.; Quirke, N. *Mol. Phys.* **1993**, *80*, 885.
(32) (a) Shevade, A. V.; Jiang, S.; Gubbins, K. E. *Mol. Phys.* **1999**, *97*, 1139. (b) Shevade, A. V.; Jiang, S.; Gubbins, K. E. *J. Chem. Phys.* **2000**, *113*, 6933.
(33) Ayyapa, K. G. *Langmuir* **1998**, *14*, 880.
(34) Macedonia, M. D.; Maginn, E. J. *Mol. Phys.* **1999**, *96* (9), 1375.
(35) Lio, A.; Charych, D. H.; Salmeron, M. *J. Phys. Chem. B* **1997**, *101*, 3800.
(36) Israelachvilli, J. *Intermolecular and Surface Forces*; Academic Press: New York, 1991.
(37) Hautman, J.; Klein, M. L. *J. Chem. Phys.* **1990**, *90*, 7483.

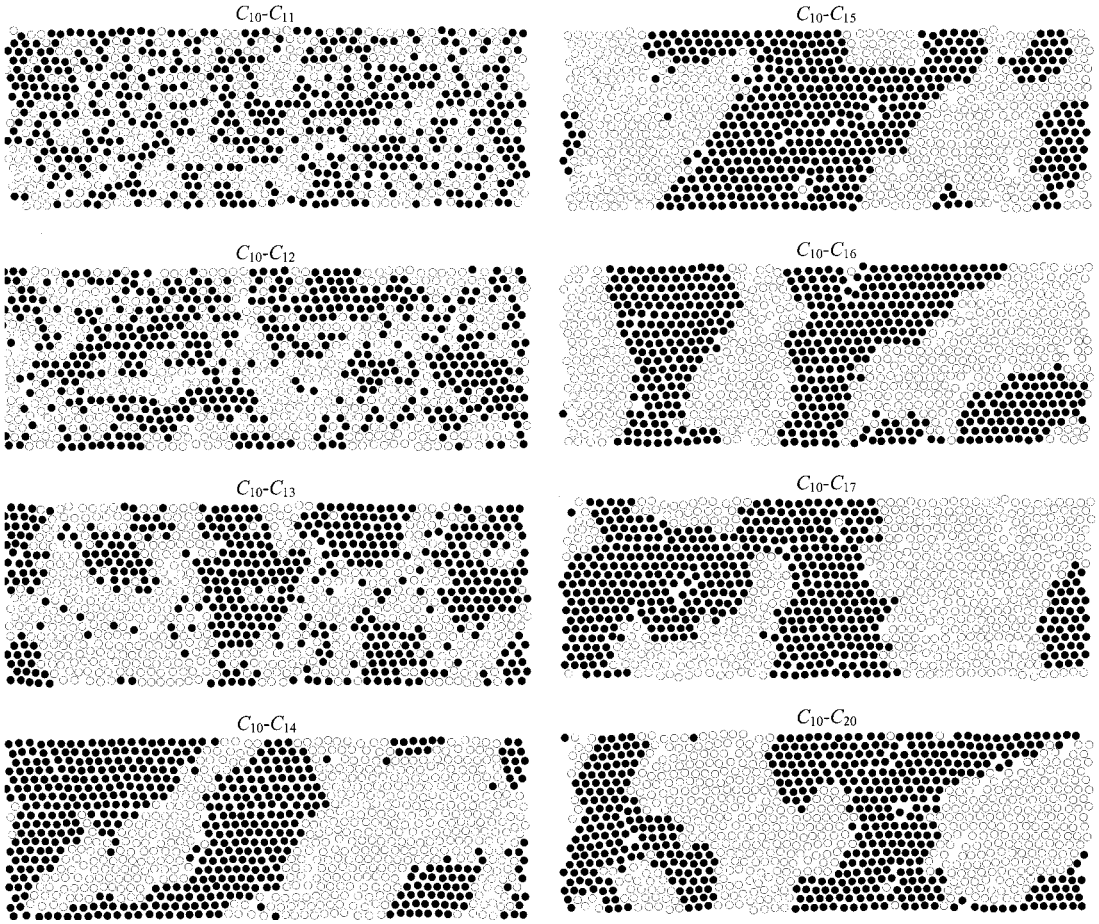

Figure 4. Headgroup configurations viewed from above for $HS(CH_2)_9CH_3-HS(CH_2)_{9+n}CH_3$ alkanethiol mixtures (where $n = 1$, 2, ..., 10) containing 1000 chains for a fixed surface composition of $x_{C10,SAM} = 0.5$ at 300 K. Open and filled circles represent the headgroups of the short and long chains, respectively.

Table 6. Equilibrium Properties of C_9-C_{10} SAMs for a Bulk Composition of $x_{C9,bulk} = 0.9$ at 300 and 373 K for 90 and 360 Chains

	300 K		373 K	
	$N = 90$	$N = 360$	$N = 90$	$N = 360$
$\langle x_{C10,SAM} \rangle$	0.55	0.53	0.44	0.47
$\langle \theta_s \rangle$ (deg)	27.19	24.41	15.33	16.35
$\langle \theta_m \rangle$ (deg)	28.13	26.18	21.76	21.94
$\langle z_{head} \rangle$ (nm)	0.240	0.240	0.242	0.240
$\langle z_{tail} \rangle$ (nm)	1.353	1.365	1.390	1.387
$\langle U_{tot} \rangle$ (kJ mol^{-1})	−170.78	−169.7	−154.94	−153.17
gauche	2.08	4.11	11.62	12.40

monolayer thickness as temperature increases for the C_9-C_{10} mixture is consistent with that from the previous study.[37]

We also studied the effect of system size for the C_9-C_{10} alkanethiol mixture by considering 360 chains and running simulations for a bulk composition of $x_{C9,bulk} = 0.9$. The system size dependence was not observed on the surface composition of the SAMs. The system size dependence on various properties of the C_9-C_{10} SAMs for a bulk composition of $x_{C9,bulk} = 0.9$ at 300 and 373 K is shown in Table 6. It can be seen that the system size has an effect on the degree of translational, orientational, and conformational order of the chains. For the system consisting of 360 chains at 300 K, it can be seen that the degree of disorder and difference between θ_s and θ_m increases with system size. There is also an increase in the density of gauche defects (about two times). The monolayer thickness as indicated by z_{tail} values shows a weak dependence on system size at 300 K. Similar observations were previously reported for pure SAM systems at 300 K.[19] System size effect is less obvious at higher temperatures.

The difference in chain length between the two components of mixed SAMs that causes phase segregation is of great interest. Mizutani et al.[21] studied phase segregation for hydrocarbon−fluorocarbon mixed SAMs where both van der Waals and dipole interactions play a role in phase segregation. For methyl-terminated mixed SAMs studied in this work, the contribution is only from van der Waals interactions. To study the effect of chain length difference on phase segregation, we simulated a system consisting of 1000 chains using CBMC simulations in the canonical ensemble at a fixed surface composition of 1:1. These simulations were carried out at 300 K for $HS(CH_2)_9CH_3-HS(CH_2)_{9+n}CH_3$ alkanethiol mixtures, where $n = 1$, 2, ..., 10. Figure 4 shows snapshots of the sulfur headgroups viewed from above for the mixed SAMs with varying chain length differences ranging from 1 to 10 carbon atoms. It can be seen that when the two components in the mixed SAMs differ by a single carbon as in the $HS(CH_2)_9CH_3-HS(CH_2)_{10}CH_3$ mixed SAMs, uniform mixed SAMs are formed. The same is true when chain length difference is increased to two carbon atoms. On further increasing chain length difference to three carbon atoms as in the $HS(CH_2)_9CH_3-HS(CH_2)_{12}CH_3$ alkanethiol mixture, it can be seen that long and short chains start to segregate into domains, which leads to phase segregation. All other systems of mixed SAMs having a chain length difference of more than three carbon atoms show clear phase segregation. This is consistent with our experiments.[25]

5. Conclusions

The preferential adsorption and phase segregation of alkanethiol mixtures on Au(111) were studied by CBMC simulations in both semigrand canonical and canonical ensembles. Simulation results in this study represent thermodynamic limit where kinetic factors are neglected. The calculated surface vs bulk composition relationship shows the preferential adsorption of long chains of mixed SAMs on the surface over in the solution. Phase segregation was found to occur when two components in mixed SAMs have a chain length difference of more than three carbon atoms. At lower temperatures, SAMs are more ordered than at higher temperatures. System size has an effect on various properties (e.g., θ_s, θ_m, and percent gauche defects) but not on surface composition. The system size effect becomes less obvious at higher temperatures.

Acknowledgment. The authors greatly acknowledge the National Science Foundation (CTS-9983895 and CTS-0092699) and the Department of Energy for financial support.

6. Appendix

A detailed description of perturbations used in CBMC simulations is discussed in section 6.1. The evaluation of Rosenbluth factors ($W^{ext}(n)$ and $W^{ext}(o)$) required in the swap, chain interconversion, and configurational-bias criteria is elaborated in section 6.2. We present a new insertion scheme based on solid−fluid biasing in section 6.3. This scheme would be useful to efficiently insert atoms strongly adsorbed on the surface, such as the sulfur atom on the gold surface in our case. The solid−fluid biasing technique along with other perturbations discussed in section 6.1 can be used to perform MC simulations in the grand canonical ensemble for the study of the adsorption phenomena.

6.1. Details of CBMC Simulations. *Translation and Rotation.* The translation step was performed in the standard way by using the center of mass.[30] For rotation, the headgroup is considered as the reference rather than the center of mass. The probability of a translation or rotation move being accepted is

$$P^{acc}_{translation/rotation} = \min[1, \exp(-\beta \Delta U(r))] \qquad (8)$$

where $\Delta U(r)$ is the change in configuration energy. Experimental and theoretical studies[18] have revealed that under physical conditions of interest, chains of the SAMs form a rotor phase, where free orientations occur around the z-axis. To replicate this phenomenon, rotation around the z-axis was kept larger than that around the x- or y-axis. For the translation move, displacements in x and y directions were kept larger than in the z direction. Translational and rotational parameters were adjusted so that the acceptance ratio for such trials was approximately 50%.

Configurational-Bias. Thorough exploration of chain conformations could be achieved by incorporating the configurational-bias move in the MC simulations involving chain molecules.[18,27] In this move, an entire chain or a part of it was discarded and then regrown unit by unit. The detailed account of this move is given below.

(i) The first step involves randomly selecting a chain and a segment to be truncated. Then, a decision whether to remove all segments above or below is also done at random.

(ii) The truncated segment is regrown according to the procedure given in the algorithm that describes the growth of a new chain (see details in section 6.2) and a normalized Rosenbluth factor of the regrown (new) chain $W^{ext}(n)$ is calculated.

(iii) The original chain is retraced from the cut segment following the steps described in the retracing algorithm of an existing chain (refer to section 6.2 for details), and a normalized Rosenbluth factor of the retraced (old) $W^{ext}(o)$ is calculated. The move is then accepted with a probability

$$P^{acc}_{configurational-bias} = \min\left[1, \frac{W^{ext}(n)}{W^{ext}(o)}\right] \qquad (9)$$

Chain Interconversion. The sampling of mixed SAMs at a fixed composition can be done by the chain interconversion move. Details of this perturbation are given below.

(i) Randomly select a long chain and a short chain from the mixed SAMs.

(ii) A portion of the long chain (equal to the difference of chain lengths between the two components) is regrown on the head of the short chain to get a normalized Rosenbluth factor $W^{ext}(n)$.

(iii) The same portion of the chain length is retraced at its original location to get a normalized Rosenbluth factor $W^{ext}(o)$.

(iv) The move then is accepted by the same criteria as given in eq 9 for the configurational-bias move.

(v) If the move is accepted, then identities of the long and short chains are changed thus keeping the total number of chains of each component in the mixed SAMs constant.

Swap. The swap technique was used for composition sampling in semigrand canonical ensemble simulations. It has been known to increase the speed of convergence in sampling the composition of a mixture and to reduce fluctuation in particle number once equilibrium is reached.[28,31−33] The swap algorithm for a chain i to be interchanged by a different chain j was performed as follows:

(i) Select a random chain i and cut it at the sulfur atom. The old chain i is then retraced starting from the carbon atom next to the sulfur atom (as discussed in section 6.2) to find the normalized Rosenbluth factor $W^{ext}(o)$.

(ii) The chain is regrown starting from the carbon atom next to the sulfur atom to obtain a new chain j with a normalized Rosenbluth factor $W^{ext}(n)$. (For molecular fluid mixtures, the new molecule is usually generated based on the center of mass of the old one.[32] In the case of SAMs, because the sulfur atom is chemisorbed on the Au(111) substrate, a new chain is regrown on the sulfur atom of the old chain.)

(iii) The swap move can be considered as a combination of deleting an old chain and inserting a new one. The probability of accepting a swap move of i to j can thus be obtained by combining the criteria for deleting an old chain i and adding a new one j [34]

$$P^{acc}_{swap,i-j} = \min\left[\frac{f_j N_i \langle W_i^{nonbond}\rangle W_j^{ext}(n)}{f_i (N_j + 1) \langle W_j^{nonbond}\rangle W_i^{ext}(o)}\right] \qquad (10)$$

where f_i and f_j are fugacities of components i and j, respectively, while N_i and N_j are the number of chains of these components. The term $\langle W_{nonbonded}\rangle$ is the average Rosenbluth factor due to the nonbonded intramolecular

interaction.[34] This is calculated during simulations. The number of j to i and i to j attempted swaps is kept equal to maintain microscopic reversibility. The acceptance probability of j to i swap is given by eq 10 with the subscripts i and j interchanged.

6.2. Evaluation of Rosenbluth Factors: $W^{ext}(n)$ and $W^{ext}(o)$. *Growing a New Chain* $W^{ext}(n)$. The insertion of sulfur atoms on the gold surface can be done by solid−fluid biasing[38] (as discussed in section 6.3) since sulfur atoms of alkanethiol chains are chemisorbed on the gold surface. The stepwise procedure for building the carbon backbone starting from any carbon atom m is as follows:

(i) A set of k trial positions denoted by $\mathbf{b} = (\mathbf{b}_1, \ldots \mathbf{b}_k)$ are generated using the valence part of the potential.[18,19] The creation of trial sites proceeds as follows: first, generate a random vector on a unit sphere and compute the internal potential energy (bond-angle bending and torsion based on the type of atom) and the corresponding Boltzmann weight for a bond directed along this vector. The vector is accepted or rejected based on the standard Metropolis criterion. If accepted, the trial site position is determined by scaling the vector to the required bond length. The procedure is repeated until the desired number of k trial sites is reached.

The internal potential energy for the second atom (atom next to the sulfur atom) in the chain is zero; hence, the second atom is created by selecting a random vector of the k trial vectors generated on the surface of a sphere. The internal potential energy for the third atom includes bond-angle bending and that for the fourth and higher atoms includes both bond-angle bending and torsion terms.[39] The computational efficiency of the simulation is decided by the choice of the k value. A lower value of k increases the probability of terminating the growth process of a chain before the desired chain length is reached. It is found that the computational time for the CBMC simulations varies linearly with k.[18] The choice of $k = 6$ used in the current simulations is in accordance with the value used for liquid alkanes.[40]

For each of these trial vectors, the nonbonded (external) energy $u_i^{ext}(\mathbf{b}_i)$ is calculated, and the position is selected with a probability

$$p_i^{ext}(\mathbf{b}_n) = \frac{\exp[-\beta u_i^{ext}(\mathbf{b}_n)]}{w_i^{ext}(n)} \tag{11}$$

where

$$w_i^{ext}(n) = \sum_{j=1}^{k} \exp[-\beta u_i^{ext}(\mathbf{b}_j)] \tag{12}$$

where contributions to the $u_i^{ext}(\mathbf{b}_n)$ term are from inter- and intra-nonbonded fluid−fluid interactions of the site i of the chain as well as from interactions with the surface.

(ii) Repeat above steps until the entire alkanethiol chain of length l is grown. The normalized Rosenbluth factor $W^{ext}(n)$ is calculated as

$$W^{ext}(n) = \prod_{i=m}^{l} \frac{w_i^{ext}(n)}{k} \tag{13}$$

Retracing an Old Chain ($W^{ext}(o)$). The retracing of an existing chain starting from any atom m of the carbon backbone is done as follows:

(i) The external energy $u_i^{ext}(o)$ (consisting of nonbonded fluid−fluid and solid−fluid contributions) of the original atom m is calculated, and then a set of k-1 trial orientations are generated (as discussed previously). Using orientations and positions of original atoms, we can calculate the Rosenbluth factor $w_i^{ext}(o)$ for atom i in the chain

$$w_i^{ext}(o) = \exp[-\beta u_i^{ext}(o)] + \sum_{j=2}^{k} \exp[-\beta u_i^{ext}(\mathbf{b}_j)] \tag{14}$$

(ii) The procedure as described above is repeated and the normalized Rosenbluth factor ($W^{ext}(o)$) for the entire chain is calculated as

$$W^{ext}(o) = \prod_{i=m}^{l} \frac{w_i^{ext}(o)}{k} \tag{15}$$

6.3. Biased Sampling Based on Solid−Fluid Potential.[38] When a fluid is adsorbed on a surface, molecules are attracted to the substrate with a solid−fluid interaction potential U_{sf}. The solid−fluid potential decays as the distance from the surface increases so that molecules will adsorb near the surface with high probability. However, in conventional simulation studies of adsorption phenomena, molecules are added randomly. The probability of a creation being accepted is usually low, especially for a large system size at low temperature. So, a biased sampling technique is used based on the insertion of the atom (sulfur atom in our case) to the solid−fluid potential. The probability of an unbiased move being accepted is given by

$$P_{move}^{acc} = \min[1, \exp(-\beta \Delta W)] \tag{16}$$

where W is the pseudo-Boltzmann distribution.[30] For a more general expression, one has

$$P_{move}^{acc} = \min\left[1, \exp\left(-\beta \Delta W \frac{P_{gen}^{old}}{P_{gen}^{new}}\right)\right] \tag{17}$$

where P_{gen}^{new} is the probability with which we generate a possible new configuration and vice versa for P_{gen}^{old}. Let us consider one specific example of a fluid adsorbed on a smooth surface, where the solid−fluid potential is only a function of distance z from the wall. One can generate a new configuration in the following two ways:

(i) Choosing the position in the z direction at random $P_{gen}^{new} = P_{gen}^{old} = 1/L$, where L is the length of the simulation box in the z direction. Thus, the acceptance rule becomes the normal Metropolis rules as in eq 16.

(ii) Choosing the position in the z direction according to the solid−fluid potential U_{sf} so that $P_{gen}^{new} \sim \exp(-\beta U_{sf,new})$ and $P_{gen}^{old} \sim \exp(-\beta U_{sf,old})$. By substituting both expressions in eq 17, the solid−fluid potential cancels out and only the fluid−fluid interaction is left in the pseudo-Boltzmann distribution.

(38) Jiang, S.; Gubbins, K. E. *Mol. Phys.* **1995**, *86*, 599.
(39) Smit, B. *Mol. Phys.* **1995**, *85*, 153.
(40) De Pablo, J. J.; Laso, M.; Suter, U. W. *J. Chem. Phys.* **1992**, *96*, 2395.

LA0108151